Biobased polyhydroxyalkanoate (PHA) membranes Structure/performances relationship

P. Tomietto, Patrick Loulergue, L. Paugam, J.-L. Audic

Biobased polyhydroxyalkanoate (PHA) membranes: structure/performances relationship

Pacôme Tomietto,[a] Patrick Loulergue,[a] Lydie Paugam [a] and Jean-Luc Audic [a]*

[a] Univ Rennes, Ecole Nationale Supérieure de Chimie de Rennes, CNRS, ISCR – UMR 6226, F-35000 Rennes, France.

** patrick.loulergue.1@univ-rennes1.fr*

Abstract

Within the current increasing environmental restrictions, biopolymers tend to replace common materials in many applications, from daily life items to process engineering facilities. Synthetic filtration membranes are also of concern. Herein, biopolymer based microfiltration (MF) membranes were produced with a polyhydroxyalkanoate (PHA), the poly(hydoxybutyrate-co-hydroxyvalerate) (PHBHV). The membranes were made by evaporation induced phase separation (EIPS) and the influence of the dope solution composition was studied by adding additives, polyvinylpyrrolidones (PVPs) and polyethylene glycols (PEGs). The nature, molecular weight and concentration of the additives were linked to the obtained microstructures. Both types of additives can increase membrane porosity by acting as pore former agent. However, interesting opposite effects were obtained in case of PEGs from 300 to 4000 g mol^{-1} where the additives were observed to act as plasticizers. The membranes performances were evaluated with pure water permeability and *E. Coli* bacteria rejection and correlated to the microstructure analyses. The performances were greatly improved by selecting the proper additive. This study leads to promising results for the consideration of PHA as new potential biomaterial intended for membrane fabrication.

Table of contents

1. Introduction

Today, membrane filtration processes are widely used by the separation industry due to their low energy requirement compared to thermal facilities. Within the membrane filtration processes, the pressure driven separations, like microfiltration (MF), ultrafiltration (UF), nanofiltration (NF) and reverse osmosis (RO) are the most industrially implemented. For example, around 80% of the desalination plants use the RO technology [1]. Among the membranes materials, polymers account for 95% of the total industrial market [2] : they are relatively cheap, cover a wide variety of thermo-mechanical properties and are easily shaped. Various polymers are now intended for membrane applications and the most used of them are mentioned in Table 1.

Table 1 : Commercially available polymers for membrane production.
RO: reverse osmosis, NF: nanofiltration, UF: ultrafiltration, MF: microfiltration, MD: membrane distillation, GS: gas separation, PV: pervaporation.

Polymer	Applications	Specificities	Polymer source / end of life
Cellulose acetate (CA)	NF, RO, UF, MF, GS	Easy processability Low cost Hydrophilic	Partially biobased / non biodegradable
Polyamides	NF, RO	pH tolerant Thermal stability Good mechanical properties	Petro-based / non biodegradable
Polyethersulfone (PES)	UF, MF	Easy processability pH tolerant Thermal stability Good mechanical properties Chlorine resistant	Petro-based / non biodegradable
Polysulfone (PSf)	UF, MF, GS		Petro-based / non biodegradable
Polyvinylidene fluoride (PVDF)	UF, MF, MD	Chemical resistance Thermal stability Good mechanical properties Hydrophobic	Petro-based / non biodegradable
Polyacrylonitrile (PAN)	UF	Chemical resistance Thermal stability Elasticity	Petro-based / non biodegradable
Polytetrafluoroethylene (PTFE)	MF, MD, GS	Chemical resistance Thermal stability Good mechanical properties Hydrophobic	Petro-based / non biodegradable
Polypropylene (PP)	MF, MD	Organic solvents resistance Good mechanical properties	Petro-based / non biodegradable
Polyethylene (PE)	MF	Organic solvents resistance Low cost Chemical resistance	Petro-based / non biodegradable
Polyvinyl alcohol (PVA)	PV	Easy processability Hydrophilic	Petro-based / biodegradable
Polyimides	NF, GS	Easy processability Chemical resistance Thermal stability	Petro-based / non biodegradable
Polyvinyl chloride (PVC)	UF, MF	Low cost Chemical resistance Thermal stability Good mechanical properties Hydrophobic	Petro-based / non biodegradable

Polysiloxanes	NF, GS, PV	Oxidative stability Good gas permeability Thermal stability Hydrophobic	Petro-based / non biodegradable
Polycarbonate (PC)	MF	Chemical resistance Thermal stability Good mechanical properties Hydrophilic	Petro-based / non biodegradable

However, as specified in Table 1, most of the polymeric membrane materials are non biobased and non biodegradable. Thus, these conventional polymers consume the limited fossil resources, create excessive untreated wastes and cause major environmental pollutions [3,4]. Hence, major efforts have been made to replace these widely used materials, including the development of biopolymers [5]. The membranes materials are no exception to this transition and the use of sustainable chemicals to make membranes is now of interest [6–10].

Among the selected biopolymers intended for membrane fabrication, cellulose based materials are widely used thanks to the cellulose abundance. They are continuously under development to still improve the membranes performances [10–13]. Nevertheless, cellulose based membranes are only partially biobased since chemical modifications of the cellulose structure are required. Polyvinyl alcohol (PVA) is a hydrophilic biodegradable polymer used for pervaporation membranes [14]. Nevertheless, it requires a crosslinking step to overcome its poor mechanical stability and this is the major research focus for its use in pressure driven processes [15]. Polylactic acid (PLA) is a biopolyester that has been considered for liquid filtration membranes due to its commercial availability and easy processing [16–19]. However, PLA production involves chemical reaction steps and this should be avoided to limit the environmental impact. Other biopolymers, directly extracted from biomass, have been investigated: alginate [20], starch [21], collagen [22], agarose [9] and κ-carrageenan [23]. They all have the drawback to be either swellable or soluble in water, hindering them to be used for water treatment applications. Besides the environmental aspect, some biopolymers have been investigated for membrane applications owing to their specific properties offering opportunities for new applications. For instance, chitosan has been considered due to its antibacterial property [10,24,25].

Apart from the above cited biopolymers, the broad family of the polyhydroxyalkanoates (PHAs) remains. PHAs are linear homo- and co-polyesters produced by bacterial fermentation and have versatile properties. As a result of the diverse production conditions, the PHAs side chain length and composition can vary [26,27], hence influencing the final thermo mechanical properties of the macromolecule [28–30]. Today, it is even possible to predict the PHAs monomers composition as a function of the selected growth media and bacteria [31]. This fact makes PHAs valuable to target special applications like for the medical field [32–34] and also for more common applications like cosmetics [35], packaging [28,36–39] or even toys [40]. Among the commercially available PHAs, the homo-polymer polyhydroxybutyrate (PHB) is the most widespread and the most used in the literature [41]. One drawback of PHB is its relatively poor mechanical properties when compared to common polymers [42]. However, the replacement of PHB by its co-polymer poly(hydroxybutyrate-co-hydroxyvalerate) (PHBHV) (or even longer-chain length PHA) (Figure 1) or its blending with (biobased) plasticizers are current solutions to overcome this issue [43]. In this study, a PHBHV is employed and is preferred to PHB due to its better flexibility."

PHAs are opening doors for sustainable applications [43] and some researchers have already thought to use them for membranes material [8,44–49].

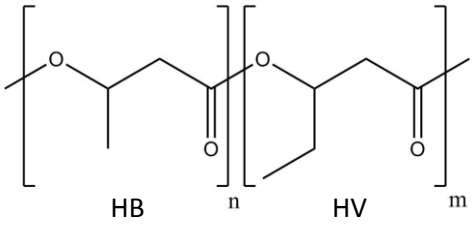

Figure 1 : Chemical structure of PHBHV

Some studies reported the use of PHAs as additives or co-material to make membranes. For instance, Nicosia *et al.* made PLA/PHB filters (with 15 wt% of PHB) for air filtration applications by electrospinning [45]. The performances were quantified by measuring the penetration of sodium chloride aerosol particles, ranging from 20 to 600 nm. The best collection efficiency was 98.5%, corresponding to the 300 nm size particles. Keawsupsak *et al.* made PLA/PHBHV blend membranes that were tested by water permeability and rejection of bovine serum albumin (BSA) measurements [8]. The performances demonstrated a permeability value of 65.2 L m^{-2} h^{-1} bar^{-1} associated with a BSA rejection of 78.7%. Finger like sub-structures were observed but there was no discussion related to the performances. Moreover, these results were obtained from a membrane with a small amount of PHBHV into a PLA matrix (1 wt% of PHBHV). Guo *et al.* fabricated composite membranes from PHB, calcium alginate and carboxyl multi walled carbon [50]. Their NF performances demonstrated a pure water flux around 35 L m^{-2} h^{-1} at 2 bar and a 98.2% rejection of brilliant blue. Moreover, the membranes exhibited good anti fouling properties. Yet, the fabrication method, combining the properties of different materials and using the electrospinning technique, still requires some efforts in upscaling applications [51].

Mas *et al.* made dense fully PHAs based membranes intended for pervaporation [47]. The membranes performances were analyzed by separation of an ethanol/water mixture. The flux varied from 0.008 to 0.027 Kg m^{-2} h^{-1} and the separation factor from 5.0 to 12.6 in favor to water permeation. Similarly, Villegas *et al.* fabricated a dense PHB based pervaporation membrane [49]. They tested the membrane for separation of methanol/methyl tertiary butyl ether (MTBE) mixtures. In the case of 40 mol% methanol/MTBE mixture, a flux of 0.392 Kg m^{-2} h^{-1} and a separation factor of 3.98 in favor to the methanol permeation were obtained. The membranes structures were not discussed. Afterwards, the same authors evaluated a modified PHA membrane by plasma polymerization with acrylic acid [48]. The authors were able to improve the separation factor up to 18.6.

So far, Mas *et al.* were the only ones having made fully PHAs based membranes for water filtration. In a first paper, the authors studied the evaporation induced phase separation (EIPS) and non-solvent induced phase separation (NIPS) conditions on the membranes performances [46]. The permeabilities varied from 50 to 1300 L m^{-2} h^{-1} bar^{-1}. The best rejection result was obtained with the least permeable membrane and was measured at 75% for dextran 2.10^6 g mol^{-1}. Nevertheless, in this case, the rejection is too low for filtration applications. Moreover, no structural analysis was performed. In a second paper, the same authors studied the influence of the EIPS and NIPS

conditions on the microstructures and membranes permeabilities [47]. Asymmetric structures were obtained with surface pores ranging from 0.25 to 2 µm. If the permeability performances were measured and went up to 600 L m^{-2} h^{-1} bar^{-1}, they were not linked to the microstructures and no rejection test was performed.

At the end, PHAs are recognized of having good potential as membrane materials [52]. Nevertheless, knowledge related to structures-performances relationship of PHAs based membranes is scarce and some efforts must be done to master it and thus to improve the performances of fully PHA based membranes.

Herein, the PHBHV has been chosen, due to its better mechanical properties compared to PHB [53], and was used for the fabrication of MF membranes. The membranes were easily made by the EIPS technique. For the first time with this type of biopolymer, the influence of different additives on the microstructure was investigated. Polyvinylpyrrolidones (PVPs) and polyethylene glycols (PEGs) of different molecular weights were added at different concentrations in the dope solution. The membranes microstructures were characterized by scanning electron microscopy (SEM), pore size distribution and overall porosity. The performances were then evaluated in terms of pure water permeability and *E. Coli* bacteria rejection from water, in order to demonstrate their potential as biobased MF membranes. Finally, the filtration performances were directly discussed according to the membranes microstructures.

2. Experimental section

2.1. Chemicals

PHBHV pellets were supplied by Tianan Biologic Material (China), under the trade name Enmat Y1000P. It was purified by dissolution in chloroform and precipitation in methanol. The white purified PHBHV powder was characterized by gel permeation chromatography (GPC) equipped with three successive columns (2 × ResiPore and 1 × PL gel Mixed C from Agilent) and a Waters UV detector working at 241nm. The molecular weight was measured at 116 000 g mol^{-1}. Differential scanning calorimetry (DSC) (TA Instruments - Q10 DSC) was used to determine its crystallinity degree, χ_c= 62%. The hydroxyvalerate (HV) monomer content was measured at 3 mol% by ^{1}H NMR analysis (Brucker 400 MHz). The latter is in accordance to what have been reported previously on this commercial PHBHV [54].

Polyethyleneglycol (PEG) 300 g mol^{-1} was supplied by VWR (U.S.); PEG 1500, 2000, 4000 and 8000 g.mol^{-1} by Sigma-Aldrich (U.S.); PEG 600 and 1000 g mol^{-1} by Alfa Aesar (U.S.); PEG 400 g mol^{-1} by Acros Organics (Belgium) and PEG 35000 g mol^{-1} by Fluka AG (Switzerland). Polyvinylpyrrolidone (PVP) 10000 and 40000 g.mol^{-1} were supplied by Sigma-Aldrich (U.S.). Chloroform (99% grade) and methanol (99.9 % grade) were supplied by Fisher Scientific (U.S.). *Escherichia Coli (E. Coli)* bacteria were used for the rejection tests. Peptone from soybean and sodium chloride were supplied by Acros Organics (Belgium). Tergitol 7 agar and TTC 12.5 mg (triphenyltetrazolium chloride) supplements were supplied by Biokar diagnostics (France). All these chemicals were used without further purification.

2.2. Preparation of PHBHV based membranes

The PHBHV based membranes were prepared by solution casting followed by phase inversion induced by evaporation. First, homogeneous dope solutions were prepared by dissolving the purified PHBHV powder and additives in chloroform under reflux for 4 hours. The different compositions of the herein studied membranes are noted in Table 2. The dope solutions were then casted at 250 µm thickness on a glass plate kept at 25°C and next left for 10 min for solvent evaporation. The obtained membranes were then soaked 5 min into 2,5 L of demineralized water to remove the remaining additives and to ensure the membrane detachment. Then, the membranes were dried by gently removing the water at the membrane surface with absorbent paper. First, they were stored for 12 hours in a desiccator under vacuum, and then finally kept under ambient conditions in a closed box.

Table 2 : References of the various fabricated membranes. Concentrations are in weight percentage (wt%) in respect to the total dope solution.

Membrane reference	PHBHV concentration	Additives	
		Nature	Concentration
PHBHV15	15%	None	
PHBHV10	10%		
PHBHV/2%PEG300	10%	PEG 300	2%
PHBHV/5%PEG300			5%
PHBHV/2%PEG8000		PEG 8 000	2%
PHBHV/5%PEG8000			5%
PHBHV/2%PEG35000		PEG 35 000	2%
PHBHV/5%PEG35000			5%
PHBHV/2%PVP10000		PVP 10 000	2%
PHBHV/5%PVP10000			5%
PHBHV/2%PVP40000		PVP 40 000	2%
PHBHV/5%PVP40000			5%

2.3. Characterization

2.3.1. Scanning electron microscopy (SEM)

The surface and cross section structures of each membrane were observed by SEM using a JSM-7100F apparatus from JEOL at an acceleration voltage of 5.0 kV and with different magnifications. For the cross section analyses, the samples were fractured after liquid nitrogen cooling. The samples were coated with a palladium/gold mixture.

2.3.2. Porosity measurements

The pore size distribution and the membrane porosity were measured by mercury intrusion porosimetry. The AutoPore IV 9500 apparatus from Micromeritics (United States) was used. The intrusion pressure range was from 17 PSI (117.10^3 Pa) to 60.10^3 PSI (413.10^6 Pa).

2.3.3. FT-IR spectroscopy

Fourier transform infrared analyses were performed with a Jasco FT/IR-4100 spectrometer equipped with an attenuated total reflection module and with a zinc selenide crystal. Spectra were done in the wavelength range of 600-4000 cm^{-1} at room temperature with 2 cm^{-1} spectral resolution and 128 scans.

2.3.4.Membranes performances

Membranes performances were evaluated by a pure water permeability measurement followed by the determination of *E. Coli* bacteria rejection.

Membranes disks of 44 mm diameter were cut with a cutting knife to fit in the filtration cell. Disks were soaked into demineralized water for 12 hours before the tests. The filtration cell was a dead-end Amicon stirred cell of 50 mL (model 5122), with a filtration area of 12.6 cm^2. A pressurized air bottle equipped with a pressure regulator was used to ensure pressurization of the system and thus establish the transmembrane pressure. For all the following steps, experiments were done under a biosafety cabinet to avoid any contamination of the samples.

2.3.4.1. Pure water permeability

All membranes were soaked in water for 24h before use. For the pure water permeability measurements, a 5L inox container, from Sartorius Stedim Biotech, was added upstream to the cell. First, the membranes were conditioned with a transmembrane pressure (TMP) of 2 bars, at 22°C, until the water flow stabilization. Then, the mean of three measures was achieved.

The pure water permeability (L_p, L m^{-2} h^{-1} bar^{-1}) was calculated from:

$$L_p = \frac{Q}{S \times TMP}$$

Where Q is the water flux (L h^{-1}), S the membrane surface (m^2) and TMP the transmembrane pressure (bar).

2.3.4.2. *E. Coli* bacteria filtration

Bacteria suspensions were prepared by making a dilution of the *E. Coli* culture broth in a maximum recovery diluent solution to give a suspension concentration of 10^4 cells per mL. The MRD solution was made by dissolving 0.9 g of peptone from soybean and 7.65 g of sodium chloride in 900 mL of demineralized water, and was then autoclaved at 121°C for 15 min. Then, 50 mL of the obtained bacteria suspension were filtered through the membrane under stirring at a TMP of 1 bar. Before collecting the first permeate sample, 10 mL of the feed solution were filtered. Then the permeate samples were collected in sterilized vials. Finally, the permeate samples were analyzed by bacteria enumeration.

To proceed to the enumeration, serial dilutions, from 10^{-1} to 10^{-4}, were done in sterilized water and were quantified in triplicate by the pour plate method. For this method, 0.1 mL of each dilution was spread in different sterile Petri dishes containing a growth solidified medium. The solidified medium is a selective and differential medium, TTC Tergitol 7 agar. Then, the plates were incubated at 37°C for 24h. Finally, the number of bacteria colonies was enumerated and reported in colony forming unit (CFU). From each Petri dish, the concentration was calculated as follow:

$$C(CFU.mL^{-1}) = \frac{CFU \times Dilution\ factor}{0.1}$$

Then, the rejection was calculated as:

$$R = \left(\frac{C_{feed} - C_{permeate}}{C_{feed}}\right) \times 100$$

Where C_{feed} and $C_{permeate}$ are respectively the bacteria concentrations, in colony-forming unit per mL (CFU.mL^{-1}), in the feed and permeate, respectively.

2.4. Hansen solubility parameters

The Hansen solubility parameters (HSP) were used to compare the affinities between the different chemicals involved in the phase inversion mechanism [55,56]. Here, it will be employed to discuss the affinities between PEGs, PHBHV and chloroform. By this method, the chemicals are described by their dispersion parameter (δ_d), polarity parameter (δ_p) and hydrogen bonding parameter (δ_h). The values of the considered chemicals are displayed in Table 3 and have been calculated using the the group contribution method and the Hoftyzer-Van Krevelen approach (detailed calculation is given in Supplementary Information S1). The last parameter introduced by Bagley *et al.* [57], δ_v, is an association of both δ_d and δ_p and is calculated as follow:

$$\delta_v = \sqrt{(\delta_d^2 + \delta_p^2)}$$

Table 3 : Hansen's parameters of PEGs, PHBHV and chloroform.

Chemical	δ_d (MPa$^{1/2}$)	δ_p (MPa$^{1/2}$)	δ_h (MPa$^{1/2}$)	δ_v (MPa$^{1/2}$)
PHBHV (3 mol% HV)	16,9	7,1	10,1	18,3
Chloroform	17,8	3,1	5,7	18,1
PEG200	16,8	5,6	16,7	17,7
PEG300	16,7	4,4	14,6	17,3
PEG400	16,6	3,7	13,4	17,0
PEG600	16,6	2,9	12	16,9
PEG1000	16,5	2,2	10,8	16,6
PEG1500	16,5	1,8	10,2	16,6
PEG2000	16,5	1,6	9,9	16,6
PEG4000	16,5	1,1	9,3	16,5
PEG8000	16,4	0,8	9,1	16,4
PEG35000	16,4	0,4	8,8	16,4

To compare the affinities of the compounds between each other, the 2D diagram plotting δ_v and δ_h was displayed [57,58].

3. Results and discussion

3.1. Effect of the PHBHV concentration on the morphology and performances

First, the MF membranes were made of PHBHV and without the addition of any additive. The influence of the PHBHV concentration on the membrane structure and performances is discussed. Experimentally, it was observed that a minimum concentration of 10 wt% of PHBHV was necessary to

obtain films with good enough mechanical properties to be handled. At lower concentrations, the obtained membranes were too thin and too fragile. Hence, two PHBHV membranes were tested and analyzed, one prepared from a dope solution with 10 wt% of PHBHV (PHBHV10) and one obtained from a dope solution with 15 wt% of PHBHV (PHBHV15). The SEM images of these two membranes are presented in Figure 2.

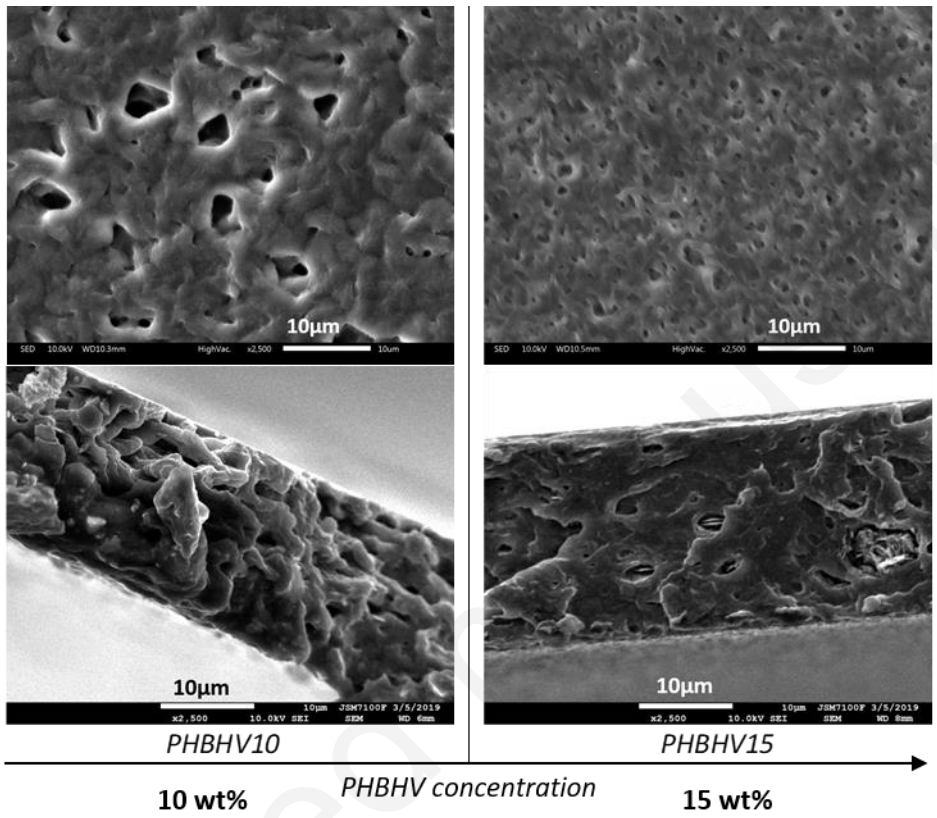

Figure 2 : SEM images of the membranes prepared with different PHBHV concentrations, 10 wt% for PHBHV10 and 15 wt% for PHBHV15. Top and bottom images are respectively surface and cross-sectional images.

Both membranes show rugged structures with pores among the surface and in the cross section. Similar structures were already observed for PHBHV films intended for vapor permeability tests [59]. For binary system, polymer/solvent, the film formation has been described by a solid-liquid phase separation owing to the polymer precipitation [60]. The pores observed on the surface (Figure 2) are explained by the formation of micro-bubbles or cracks during the drying process as previously described for the formation of porous PHA films intended for bone and skin regeneration [61].

The membranes thicknesses, porosities and performances are reported in Table 4.

Table 4 : Structural properties and filtration performances of the PHBHV membranes. Influence of the PHBHV concentration.

Membrane	Membrane thickness	Porosity	L_p	*E. Coli* Rejection

	(µm)	(%)	(L m^{-2} h^{-1} bar^{-1})	(%)
PHBHV10	18.0 ± 0.6	9.0 ± 0.5	4.2 ± 2.6	95,00 ± 2.80
PHBHV15	22.4 ± 0.2	5.0 ± 0.3	0.2 ± 0.1	-

The pores observed on Figure 2 seem to be more significant for the membrane made with the lower PHBHV concentration, PHBHV10. It is confirmed by the higher measured porosity of the PHBHV10 membrane compared to the PHBHV15 membrane (Table 4). Indeed, a lower dope solution concentration, and hence a lower solution viscosity, tends to increase the solvent evaporation rate [62]. As a consequence, the molecular chains have less time to flow and the structure is entrapped faster. It results in a structure with more trapped micro-bubbles and defects, leading to a more porous membrane. The lower thickness of PHBHV10 membrane is simply explained by a lower amount of polymer per surface unit.

As a result of the microstructures change, a major variation is observed on their filtration performances. The PHBHV10 membrane exhibits higher pure water permeability, 4.2 L m^{-2} h^{-1} bar^{-1}, compared to the PHBHV15 membrane, 0.2 L m^{-2} h^{-1} bar^{-1}. It is in accordance with the microstructural analyses: the most permeable membrane also being the most porous and the thinnest. Besides, the PHBHV10 membrane shows an *E. Coli* rejection of 95,00%. It was not possible to determine the *E. Coli* rejection of the PHBHV15 membrane because of its very low permeability. Regarding its better filtration performances, the PHBHV concentration of 10 wt% appears to be the best. However, even at this concentration, the membrane properties are not satisfactory. The effect of additives on the membrane structure and performances has thus been evaluated to improve the membrane properties.

3.2. Effect of additives on the morphology of membranes

With the aim of improving the overall porosity of the membrane and its permeability, different additives, PVPs and PEGs, were added into the dope solution at different concentrations. These additives have already been widely used as pore former agent for the membrane fabrication [12,60,63–67]. Indeed, from a thermodynamic point of view, the additives can act as a non-solvent and consequently tend to increase the membrane porosity [65]. On the other hand, from a kinetic point of view, the additives can decrease the phase inversion rate, by increasing the viscosity of the dope solution, which results in an increased coarsening time that favors the formation of larger pores [60].

3.2.1. Effect of PVP

PVP is a common additive employed for the membrane fabrication [12,64]. Additionally to its pore former effect, this additive is also used as hydrophilic additive, thus improving the membrane water permeability [68]. The molecular weights of the PVPs used for this study are 10000 and 40000 g mol^{-1}.

Figure 3 represents the membranes SEM images. The SEM images of the membranes show symmetric sponge like structures. Membranes surfaces are smooths with visible pores. These pores are smaller than those observed without any additive (PHBV10, Figure 2).

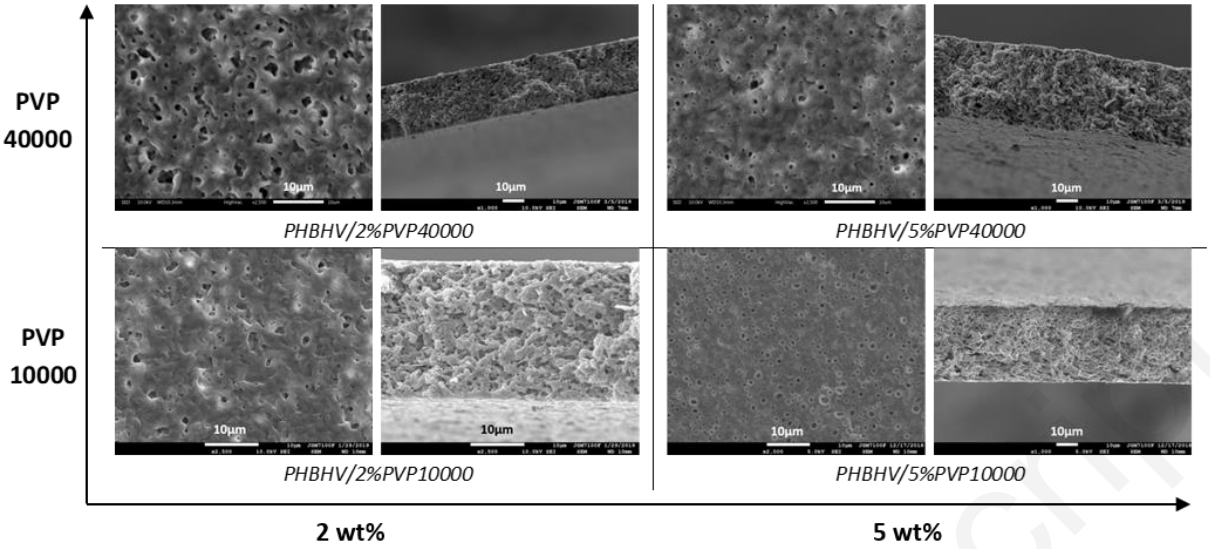

Figure 3: SEM images of the membranes prepared with different PVPs molecular weights and concentrations. Surface on the left, cross section on the right. PVPs concentrations in weight percent into the dope solution. With a constant PHBHV concentration of 10 wt%.

Figure 4 displays the membranes pore size distribution. The results obtained by measuring the pore size distribution displays a volumetric distribution peak centered around a value greater than 1 µm (mean pore size 1.71 µm, Table 5) for the PHBHV10 membrane. By adding PVP, the peak shifts to smaller pore size. The average pore diameter of membranes containing PVPs vary from 0.53 to 0.89 µm.

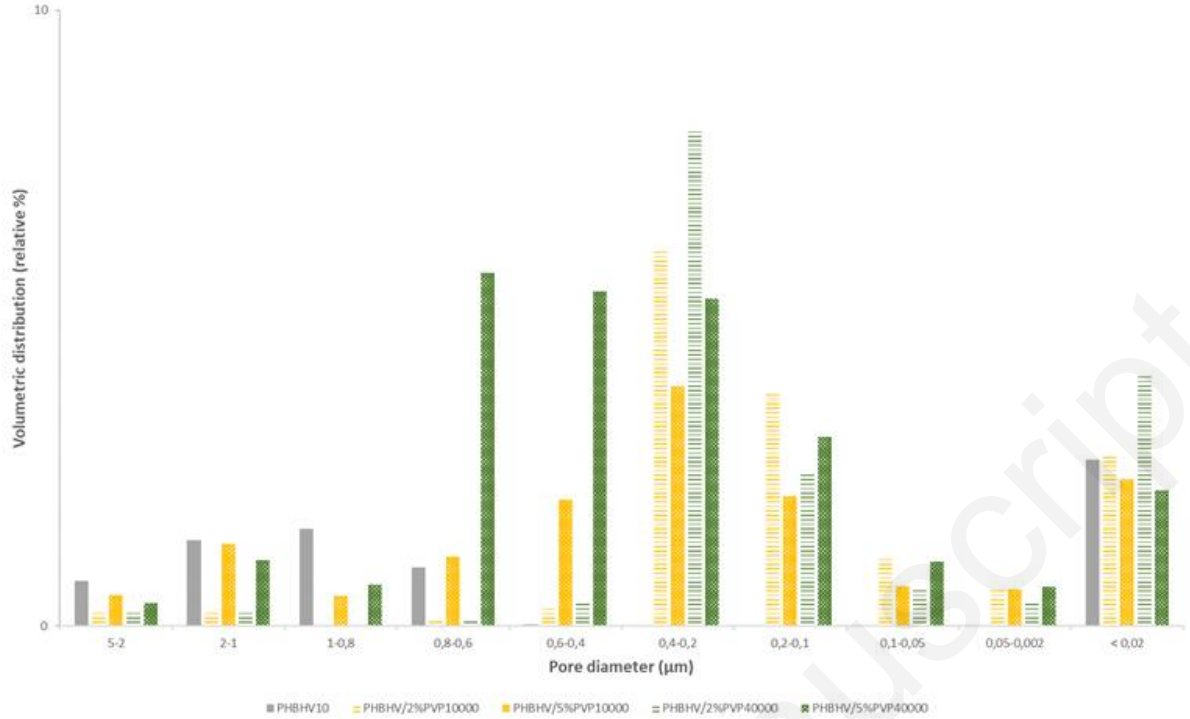

Figure 4 : Pore size distribution of the various membranes made with PVPs as additives.

In this case of ternary system, polymer/solvent/additive, the phase inversion mechanism occurs through a liquid-liquid demixing, between a polymeric rich phase and a polymeric lean phase, followed by solidification [60,69]. The polymeric rich phase is made of a majority of PHBHV and a minority of solvent while the polymeric lean phase is made of the additive (acting as non-solvent) and the remaining solvent. In the early stage of the liquid-liquid demixing, a co-continuous structure is firstly formed but then the coarsening effect leads to fragmented particles of the polymeric lean phase and then spherical particles. The later would make the final pores of the membrane. Meanwhile, the polymeric rich phase would solidify yielding the final membrane matrix.

This mechanism is fundamentally different from the solid-liquid demixing described previously for the membranes without additive. Hence, while the pores of PHBHV10 membrane resulted from trapped micro-bubbles and defects here they result from a homogeneous growth of a liquid polymeric lean phase. Thus, it explains the change of the pore size when PVP is added to the dope solution. In addition, by adding PVP, the dope solution viscosity can be increased thus decreasing the phase inversion rate [12] and preventing the formation of defects by giving more time for the macromolecular chains rearrangement.

Then, the increasing of additive concentration tends to shift the volumetric distribution to higher pore size. Indeed, because the viscosity increases with PVP concentration [12], the coarsening time too thus leading to the formation of bigger pores [60]. Furthermore, the main distribution peak is even wider when the concentration of additive is higher, what means a wider pore size dispersity. Asymmetric membranes with wide pore size distributions are due to an additive concentration

gradient across the thickness during the evaporation and are favored with the increasing of the non-solvent concentration [69,70].

Two other structural parameters, the membrane thickness and porosity, are reported in Table 5.

Table 5 : Thickness and porosity of the different membranes made with PVPs as additives.

Membrane	Membrane thickness (µm)	Porosity (%)	Mean pore size (µm)
PHBHV10	18.0 ± 0.6	9.0 ± 0.5	1.71
PHBHV/2%PVP10000	25.6 ± 0.3	15.9 ± 0.8	0.53
PHBHV/5%PVP10000	35.0 ± 0.3	16.1 ± 0.8	0.89
PHBHV/2%PVP40000	23.7 ± 0.3	17.4 ± 0.9	0.61
PHBHV/5%PVP40000	36.0 ± 0.8	26.1 ± 1.3	0.61

The addition of PVP10000 or PVP40000 increases the porosity compared to the PHBHV10 membrane. This confirms the porogeneous effect of PVP10000 and PVP40000. Since they could act as non-solvent, adding these compounds or increasing their concentration, increase the polymeric lean phase volume and hence the final membrane porosity. In case of PVP10000, the addition of 2 wt% or 5 wt% leads to similar porosity values, respectively 15.9% and 16.1%, while the thickness increases with the concentration. The fact that the thickness increases with the concentration without influencing the porosity would indicate that between 2 and 5 wt% the PVP10000 mainly remains in the PHBHV matrix. Meanwhile, in case of PVP40000, increasing the concentration tends to increase the membrane porosity and thickness. Hence, it could be stipulated that PVP10000 acts more like a plasticizer within the range of 2 and 5 wt% but PVP40000 continue to act as a pore former agent within that concentration range.

To highlight the plasticizing effect as a function of the PVP molecular weight, the membranes chemistry was analyzed by ATR-FTIR and compared to the PHBHV10 membrane. Figure 5 gives the FTIR spectra for PHBHV10 and membranes containing PVP10000. The main bands of PHBHV10 are assigned to C-O-C asymmetric stretching (1178 cm^{-1}), C-O stretching (1228 and 1280 cm^{-1}), C-O-C asymmetric stretching (1178 cm^{-1}), C-H bending (1379 and 1457 cm^{-1}), C=O stretching (1720 cm^{-1}) and C-H stretching (2930 and 2970 cm^{-1}). These bands are in accordance with what was previously observed in the literature [71]. For PHBHV/5%PVP10000 and PHBHV/5%PVP40000 membranes a new band emerges at 1650 cm^{-1}. This band refers to the C=O amide bond and reveals the presence of remaining PVP into the membrane matrix [72].

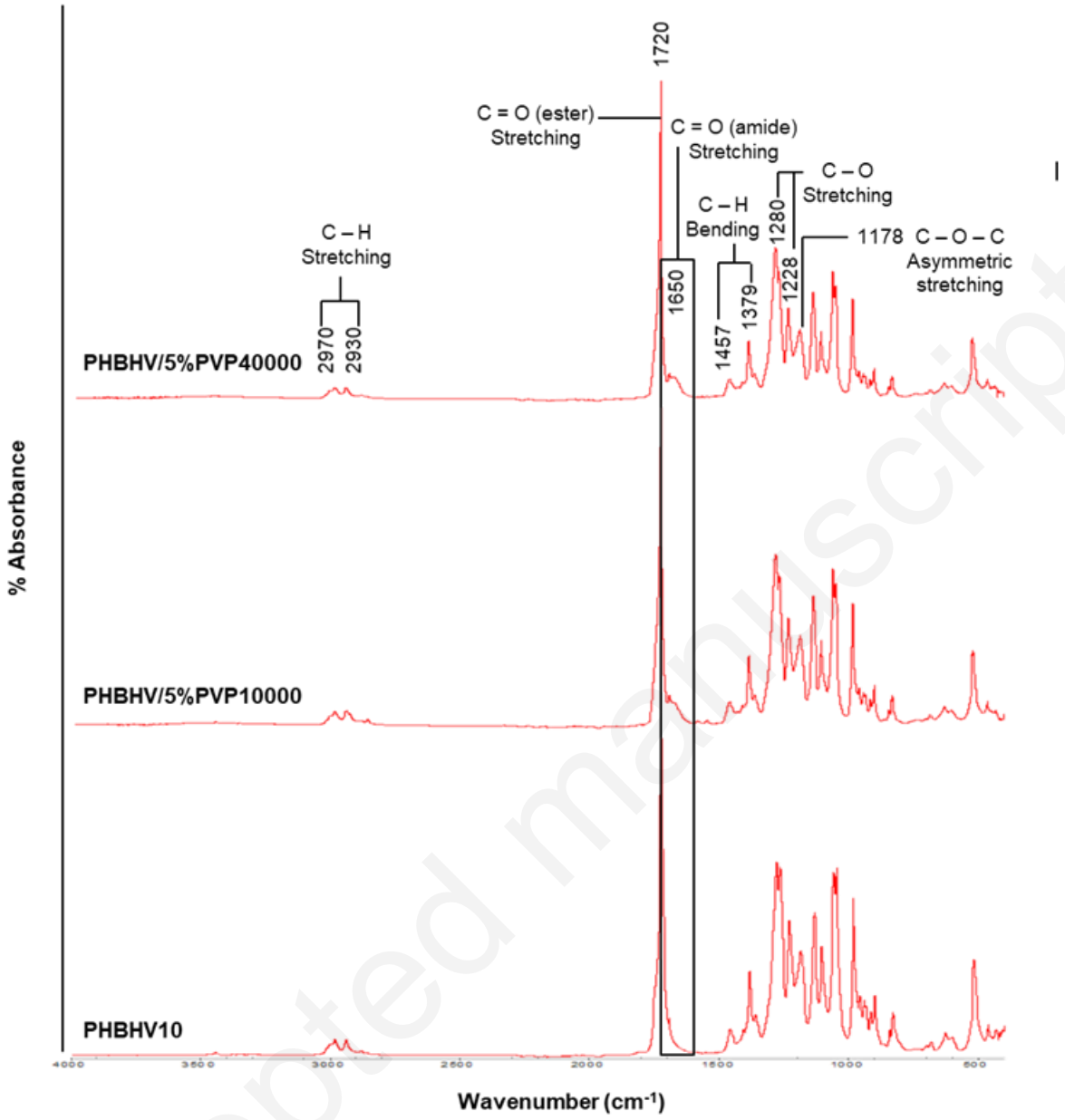

Figure 5 : Typical FTIR spectra of different membranes with or without PVP.

A method has been developed to quantify the amount of remaining PVP into the membrane, in respect to the pure membrane PHBHV10. This method is based on the ratio calculation between the band at 1650 cm^{-1}, attributed to PVP, and the band at 1720 cm^{-1}, attributed to PHBHV. The ratio of remaining PVP was calculated as follow:

$$\phi_{PVP} = \left(\frac{A_{1650}}{A_{1650} + A_{1720}}\right) \times 100$$

The calculation was made for all the membranes with PVP10000 and PVP40000 prior to membrane filtration performance evaluation (i.e. after membrane soaking into water for 24h). Then, the results

obtained for ϕ_{PVP} are correlated to the initial amount of PVP introduced into the dope solution, see Figure 6.

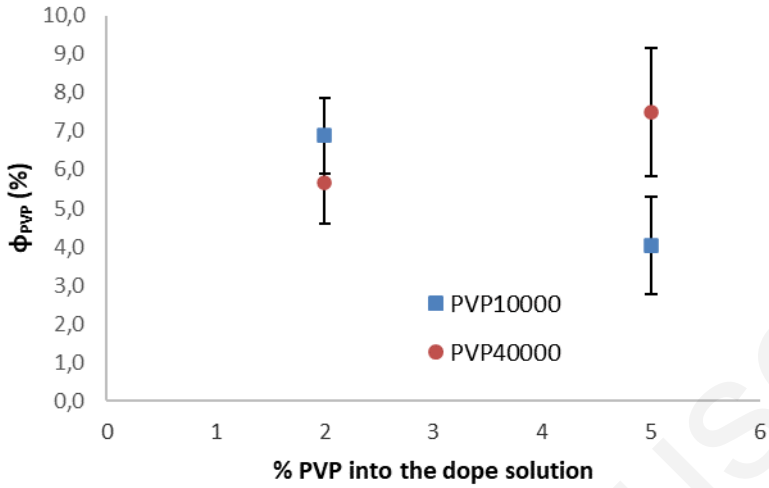

Figure 6: ϕ_{PVP} as a function of the PVP concentration into the dope solution.

The peak ratio, ϕ_{PVP} was found to be in the range 4.0 ± 1.3 and 7.5 ± 1.3 % for all membranes. These results ~~also~~ support the fact that the additive is never completely leached out from the PHBHV matrix, what has been previously reported [73]. Actually, PVP has already been blended with PHA in order to improve the thermal properties of PHA films [74], hence confirming the compatibility between these two polymers. In addition, no additional leaching of the additive was observed during membrane uses (see supplementary material S2). In addition, no influence of the initial PVP concentration in the dope solution was observed.

The membranes performances are shown on Figure 7.

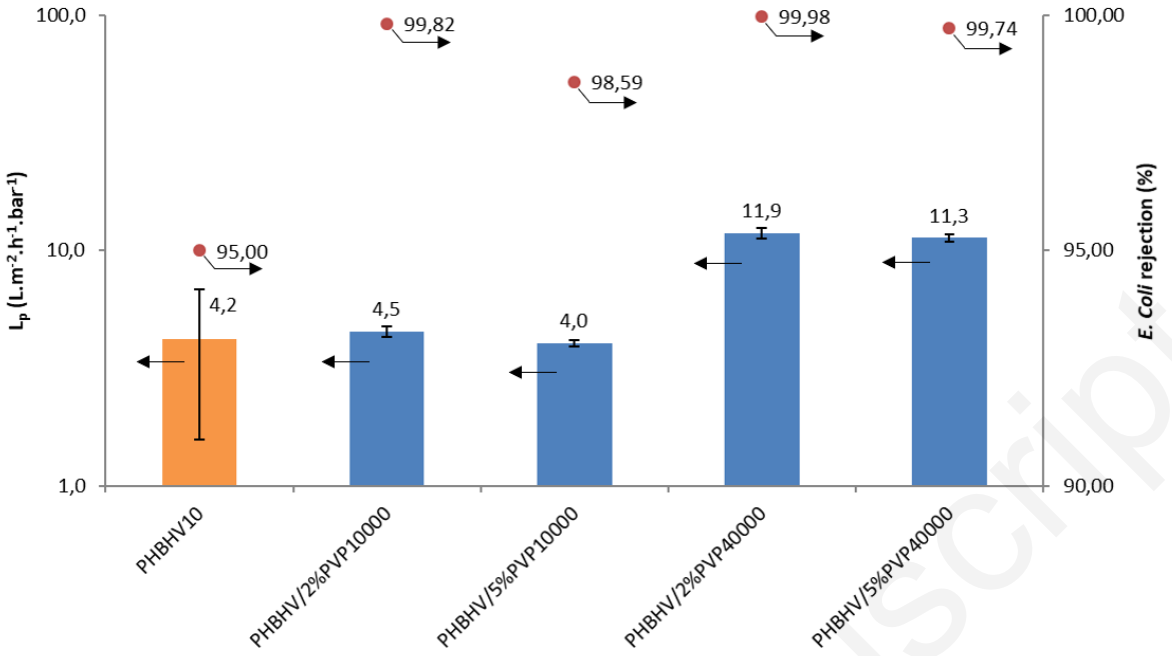

Figure 7 : Pure water permeability and *E. Coli* rejection of the PHBHV membranes with different PVPs as additives.

The addition of PVP10000 or PVP40000 improved the *E. Coli* rejections to values over 98,5%. Indeed, when PVP is added, it was previously observed on Figure 4 that the pore size distribution was decreased from 1 µm to values ranging between 0.2 µm and 0.8 µm. Knowing that the *E. Coli* bacteria have a typical size of 1 to 3 µm [75], it could explain the much better rejections of membranes with PVP. The permeabilities where not improved with the addition of PVP10000 but were improved by factor three with PVP40000.

In microfiltration, membrane permeability depends on membrane structural parameters such as membrane thickness or membrane porosity. In our case, it was observed that the permeabilities are correlated to the membranes porosities (Figure 8) but no trends was found between the membrane permeability and its thickness (See supplementary material S3). At similar porosities values, case of membranes PHBHV/2%PVP10000 and PHBHV/5%PVP10000, similar permeabilities were measured. It seems that a higher porosity tends to increase the permeability as observed for PVP40000. Nevertheless, the permeabilities were not improved between PHBHV10 membranes and PVP10000 membranes, despite the increased porosity. It could be explained by the decrease of the pore size distribution when PVP10000 is added, presumably leading to less inter connected pores and hence having an opposite effect on the permeability. Difference in pore tortuosity could also contribute to explain this observation.

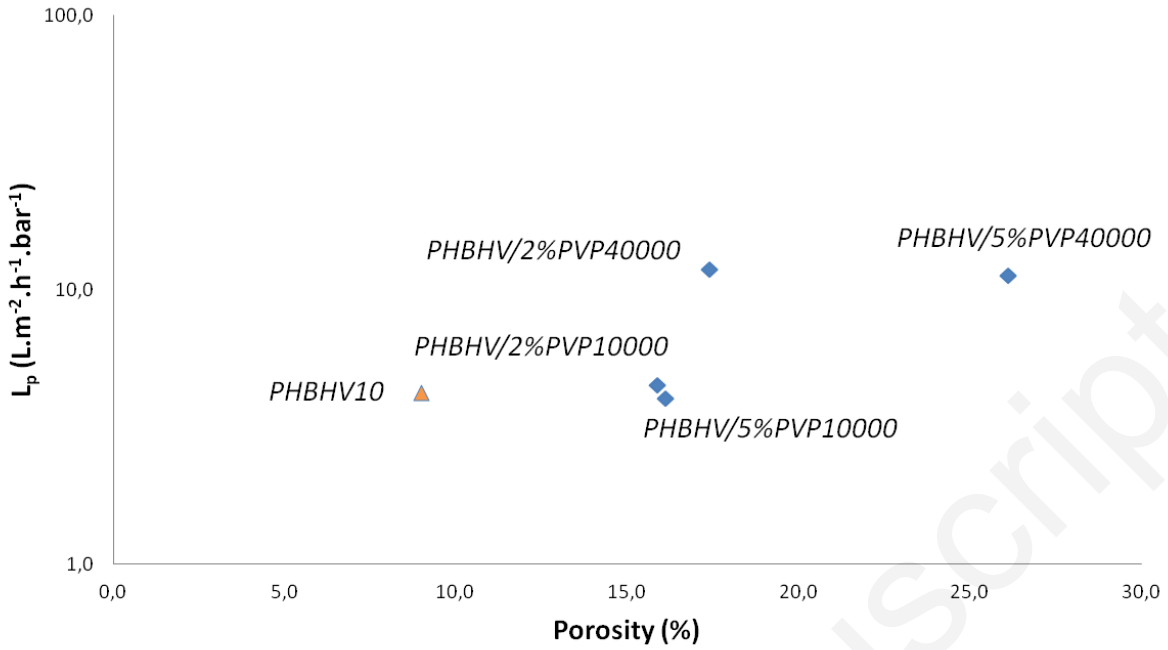

Figure 8 : Pure water permeability as a function of the membrane porosity. For membranes with PVPs as additives.

Finally, adding PVP in membranes made by EIPS tends to decrease the pore size distribution and increase the overall porosity of the membrane matrix, resulting in better rejection behaviors and slightly better permeabilities. Nevertheless, due to low membranes porosities, the permeabilities were still very low. Hence, another alternative additive, the PEG, was further investigated to improve the PHBHV based membranes performances.

3.2.2.Effect of PEG

If PEG is less commonly used for the membrane fabrication, it has already been described as a pore former agent and a hydrophilic additive in order to increase the membrane permeability [76].

3.2.2.1. Effect of the PEG molecular weight on the membrane porosity

As it was shown with PVP, a part of the additive stay in the final membrane, potentially acting as a plasticizer, in parallel to the pore former effect. For PEGs, this effect has already been reported by Xu *et al.* [77]. The authors demonstrated the macrovoid suppressor effect of PEG600 on polyetherimide membranes and showed that PEG remained in the membrane and acted as a plasticizer. Moreover, PEGs have already been intensively used as plasticizers for PHA based materials [78,79]. Hence, it could be expected that some PEGs will be more plasticizers than pore former agents. In order to select the best pore former PEG, the influence of the PEG molecular weight on the final membrane structure was firstly investigated. Different PEGs, with molecular weight ranging from 300 to 35000 g.mol^{-1}, were added into the dope solution containing the PHBHV. The dope solution concentrations are fixed at 10 wt% of PHBHV, 2 wt% of PEG and 88 wt% of solvent. The membrane porosity is presented as a function of the additive molecular weight on Figure 9.

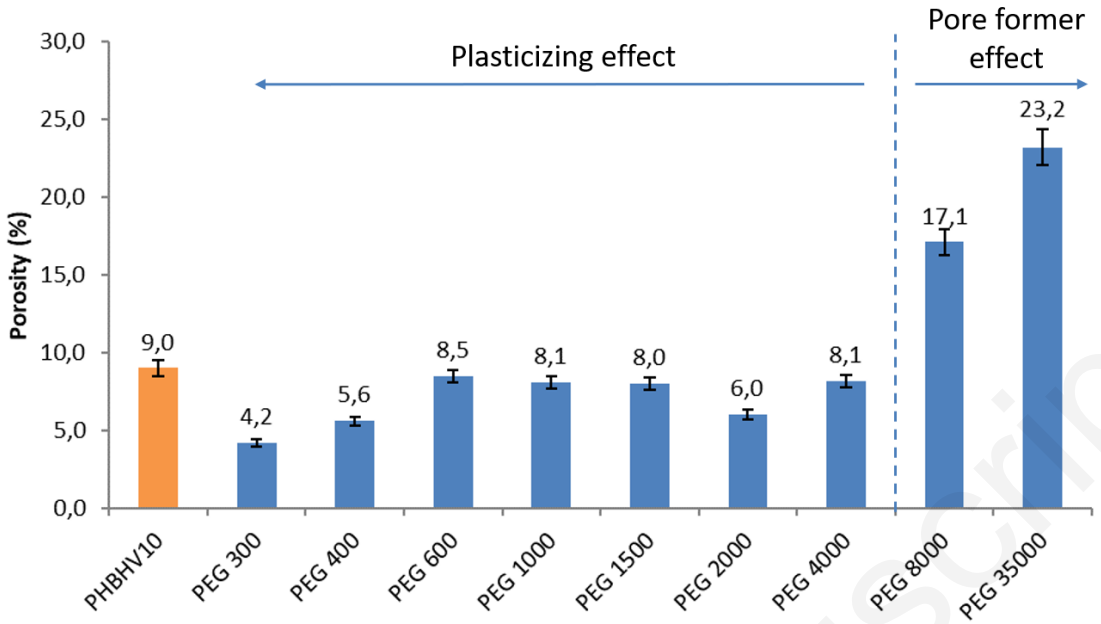

Figure 9: Membrane porosity as a function of the PEG molecular weight. The reference membrane is PHBHV10.

The membrane porosity is strongly influenced by the molecular weight of PEG. At a PEG concentration of 2 wt%, for molecular weights of 4000 g mol^{-1} or below, the presence of additive leads to lower porosities or of the same order of magnitude than the PHBHV10 membrane. It suggests that these PEGs do not act as a non-solvents and do not increase the porosity. It can be noticed that, in previous studies dealing with PHBHV/PEG blends, only PEGs with molecular weights below 4000 g mol^{-1} were studied [78,79]. In the present work, PEGs of 8000 or 35000 g mol^{-1} significantly increase the porosities thus implying their non-solvent effect. These high molecular weight PEGs act as pore former agents. It has to be kept in mind that the nature of the effect of the additives (i.e. plasticizer or pore former) can also depends on the additive concentration.

The chemical affinities between PEGs, PHBHV and chloroform can be approached using the Hansen's solubility parameters (HSP). The affinity between two chemicals can be predicted by comparing their respective HSP and the more these parameters are closed, the higher is their affinity. Since the effects of δ_d and δ_p are similar, it has been reported that plotting the 2D diagram δ_v-δ_h is a relevant easy way to represent the molecular interactions [57,58]. On Figure 10, the δ_v-δ_h diagram represents the PEGs points at different molecular weights, PHB and chloroform. The closer are the points on the diagram, the higher is the predicted affinity. Considering that the PHBHV used for these experiments has only 3 mol% of HV content, it is here assumed that PHB represent well the overall chemical structure of the employed PHBHV. In the literature, the HSP of PEGs were determined only for liquids [80], that is why only PEGs from 200 to 600 g mol^{-1} are displayed on Figure 10.

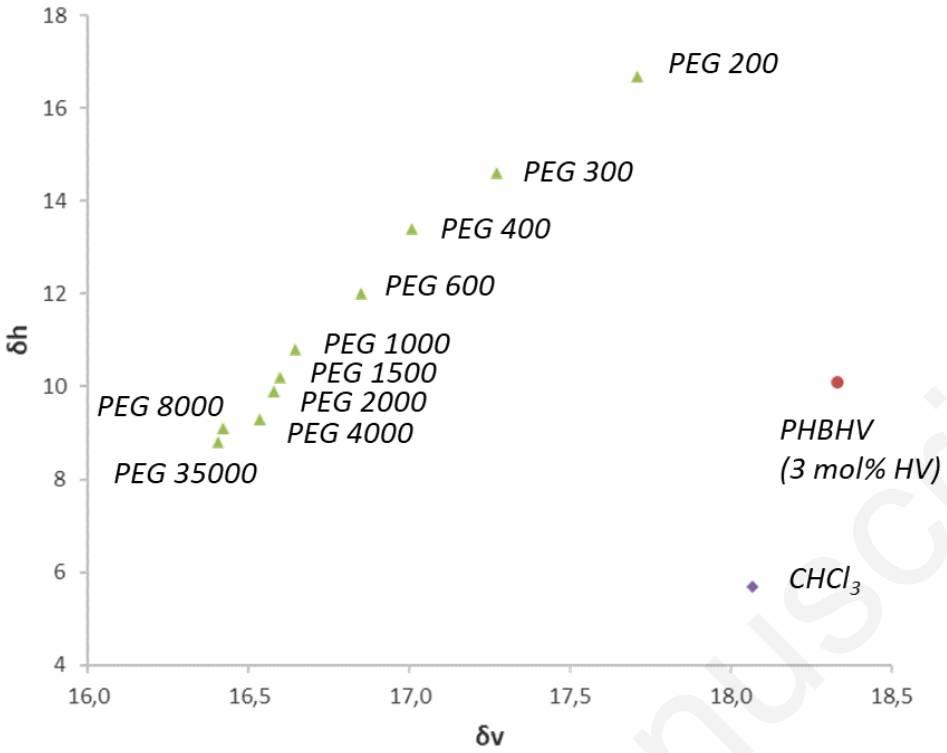

493

494 **Figure 10 : δ_v-δ_h diagram for PHBHV, chloroform and various PEGs.**

495

496 As observed on Figure 10, the position of the PEG on the δ_v-δ_h diagram depends of its molecular
497 weight and this phenomena was previously reported by Liu *et al.* [80]. Indeed, the HSP of PEG
498 depend of the OH end-groups, which are inversely proportional to the molecular weight and highly
499 contribute to the hydrogen bounding parameter (δ_h). However, it could be expected that this
500 evolution would stop at a point where the OH end groups effect would be negligible compared to the
501 entire molecule.

502 Regardless of their molecular weight, the affinity between PEGs and PHBHV is higher than the one
503 between PEGs and chloroform. In that sense, it predicts that, during the phase separation, PEGs
504 preferentially go into the polymeric rich phase without acting as a non-solvent. Then, it would not
505 contribute to the formation of pores and would even lower the porosity by potentially improving the
506 chain mobility. So that would explain the lowered porosity, observed on Figure 9, when PEGs 300 to
507 4000 g mol^{-1} were added.

508 However, the addition of PEG 8000 and PEG 35000 g mol^{-1} give more porous structures, while they
509 may also have good affinities with PHBHV. Here, it may be due to another aspect: the steric
510 hindrance. Indeed, the Hansen's parameters do not consider the steric hindrance of the molecule. It
511 was demonstrated that besides the chemical interactions, the steric hindrance is playing an
512 important role in the prediction of the compounds mixing [81]. By increasing the molecular weight,
513 the PEG increases its length and reduces its chains mobility. There is a point where the steric
514 hindrance is too high to allow the chains entanglement between PEG and PHBHV. That is why, for
515 PEG8000 and PEG35000, PEG and PHBHV are not miscible anymore and the PEGs will mainly act as
516 non-solvent and hence as a pore former agent to give membranes with higher porosities.

At the end, from the experimental porosity data, it can be argued that PEG 8000 and 35000 g mol^{-1} are the best pore former agents among the various PEGs investigated. Thus, PEG8000 and PEG35000 are selected for the rest of the study. Nevertheless, Zhao *et al.* previously reported the importance of the additive concentration to get the pore former effect [82]. At low concentrations the additive can disperse in the polymer matrix without influencing the membrane porosity. Hence, PEG300 will also be kept to see if it could be pore former at a higher concentration.

3.2.2.2. Effect of the concentration

Once the pore former PEGs are selected, similarly to what was performed with PVP, the effect of their concentrations on the membrane microstructure and performances will be analyzed. 2 wt% or 5 wt% of PEG was added in the dope solution containing 10 wt% of PHBHV. It has to be mentioned that, at higher concentration, the films were either too fragile to be tested in filtration application or visually heterogeneous, thus it was decided to focus only on these two different values of additives concentration. The SEM images of the different membranes are shown on Figure 11 and the pore size distributions are displayed on Figure 12.

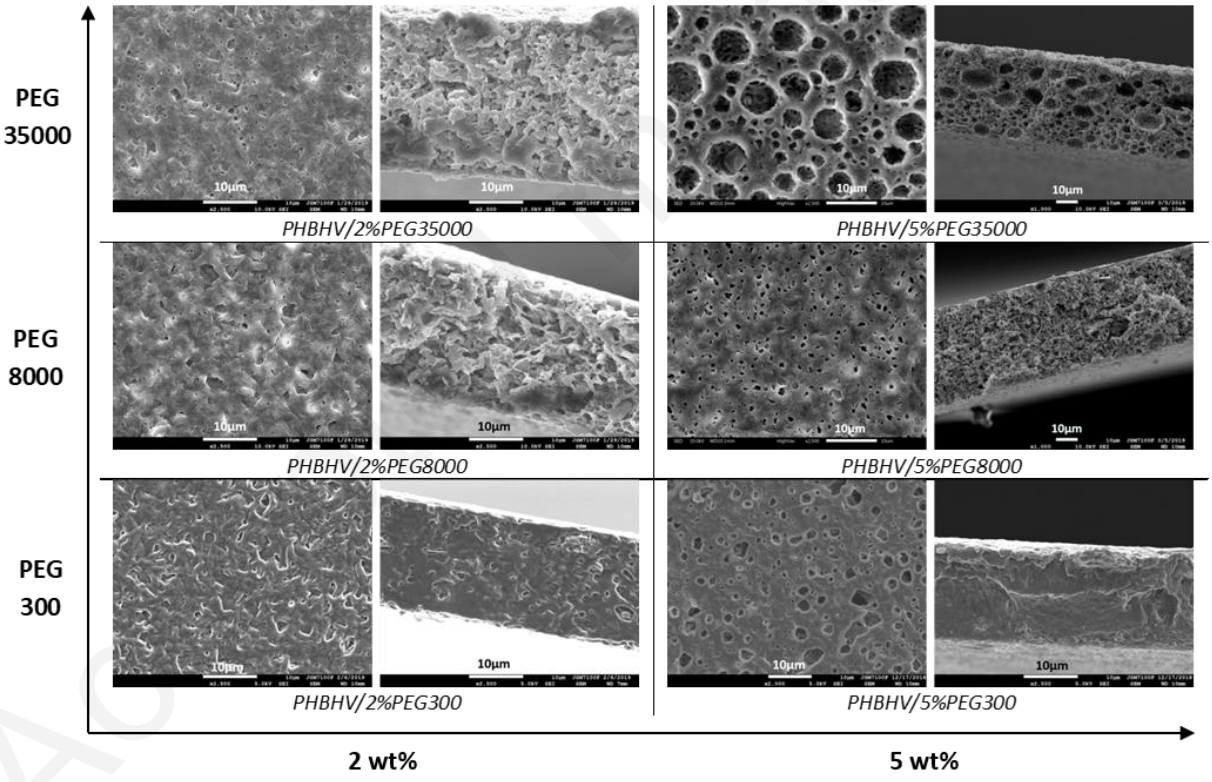

Figure 11 : SEM images of the membranes prepared with different PEGs molecular weights and concentrations. Surface on the left, cross section on the right. PEGs Concentrations in weight percent into the dope solution. With a constant PHBHV concentration of 10 wt%.

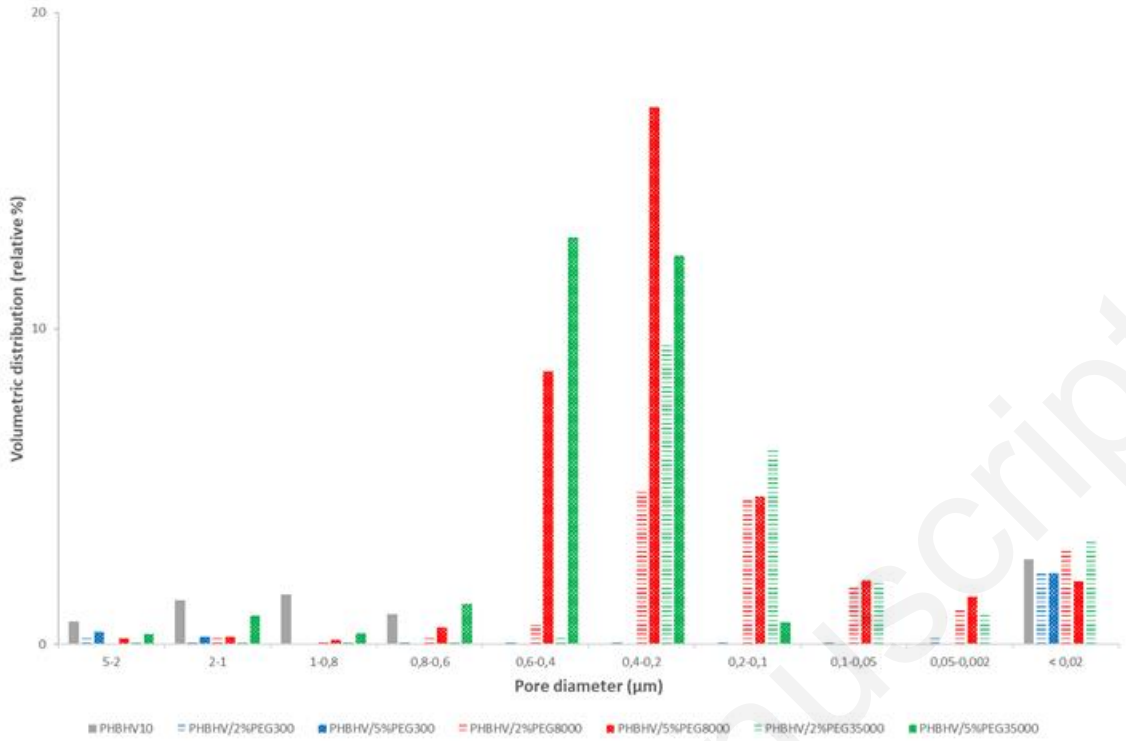

536

537 **Figure 12 : Pore size distribution of the various membranes made with PEGs as additives.**

538

539

540 Major differences on the microstructure are displayed between membranes with PEG300 and
541 membranes with other PEGs. Membranes with PEG300 seem to show closed pores while the others
542 membranes have sponge like structures, suggesting the non pore former effect of PEG300. Then, the
543 PHBHV/5%PEG35000 membrane visually presents bigger spherical pores, especially at the middle of
544 the cross section. This clearly reflects the late stage of the liquid-liquid demixing, the coarsening of
545 the polymeric lean phase yielding to spherical particles [60,69]. Because this membrane was made
546 with the highest PEG molecular weight, PEG35000, and the highest PEG concentration, 5%, the
547 solution was the most viscous and hence the one with the longer coarsening time.

548 Looking at the pore size distributions and considering membranes with PEG8000 and PEG35000, the
549 distribution peak shift to smaller pores diameters compared to membrane PHBHV10. The main peaks
550 of membranes with PEG8000 and PEG35000 vary from 0.2 to 0.6 µm (average pore size in the range
551 0.26-0.59 µm) while the peak of PHBHV10 membrane is greater than 1 µm. This trend was previously
552 observed for membranes containing PVP and was explained by the change of the phase inversion
553 mechanism.

554 Then, the increasing of additives concentration tends to shift the volumetric distribution to higher
555 pore size but also wider the distribution. Again, the same observations were made with PVP10000
556 and PVP40000. Because the viscosity increases with the additive concentration [12], the coarsening
557 time too and leads to the formation of bigger pores [60]. As explained above, the wider pore size
558 distribution can be explained by an additive concentration gradient across the thickness during the

559 evaporation which is favored with the increasing of the non-solvent concentration [69,70]. In that
560 case, PEG8000 and PEG35000 are the non-solvents.

561 Concerning the PEG300 as additive, it can be noticed that membranes with 2 wt% and 5 wt% do not
562 show any particular volumetric pore distribution in respect to PHBHV10 membrane. Again, it
563 confirms that PEG300 is not a pore former, whatever the concentration, but also hinders the
564 formation of trapped micro-bubbles or defects.

565 The effects of the additives on the membrane porosity and thickness are displayed in Table 6.

566 **Table 6: Thickness and porosity of the different membranes made with PEGs as additives.**

Membrane	Membrane thickness (µm)	Porosity (%)	Mean pore size (µm)
PHBHV10	18.0 ± 0.6	9.0 ± 0.5	1.71
PHBHV/2%PEG300	20.1 ± 0.2	4.2 ± 0.2	1.49
PHBHV/5%PEG300	17.7 ± 0.3	3.9 ± 0.2	2.45
PHBHV/2%PEG8000	25.8 ± 0.4	17.1 ± 0.9	0.26
PHBHV/5%PEG8000	42.3 ± 0.4	37.4 ± 1.9	0.40
PHBHV/2%PEG35000	29.5 ± 0.8	23.2 ± 1.2	0.37
PHBHV/5%PEG35000	42.0 ± 0.8	29.3 ± 1.5	0.59

567

568 The addition of PEG8000 or PEG35000 increases the porosity compared to the PHBHV10 membrane,
569 and a higher PEG concentration leads to higher porosities. These additives act as non-solvents, so
570 increasing their concentration increases the polymeric lean phase volume and hence the final
571 membrane porosity. Besides, the thickness increases with the porosity, what makes sense since the
572 volume of void increases too. And, concerning PEG300, with 2 wt% or 5 wt%, the membrane porosity
573 is decreased so that finally confirms the non porogeneous effect of PEG300.

574 Contrary to the membranes with PVPs, the FTIR technique was here not accurate to highlight the
575 remaining amount of PEG in the final membrane because the typical vibrational bands from PHBHV
576 overlap the bands from PEG.

577 As a consequence of the membranes microstructures changes, the membranes performances were
578 improved (Figure 13). In case of membranes with PEG300, the low porosities lead to very low pure
579 water permeabilities (below 1 L m^{-2} h^{-1} bar^{-1}) so that the *E. Coli* rejection was not tested.

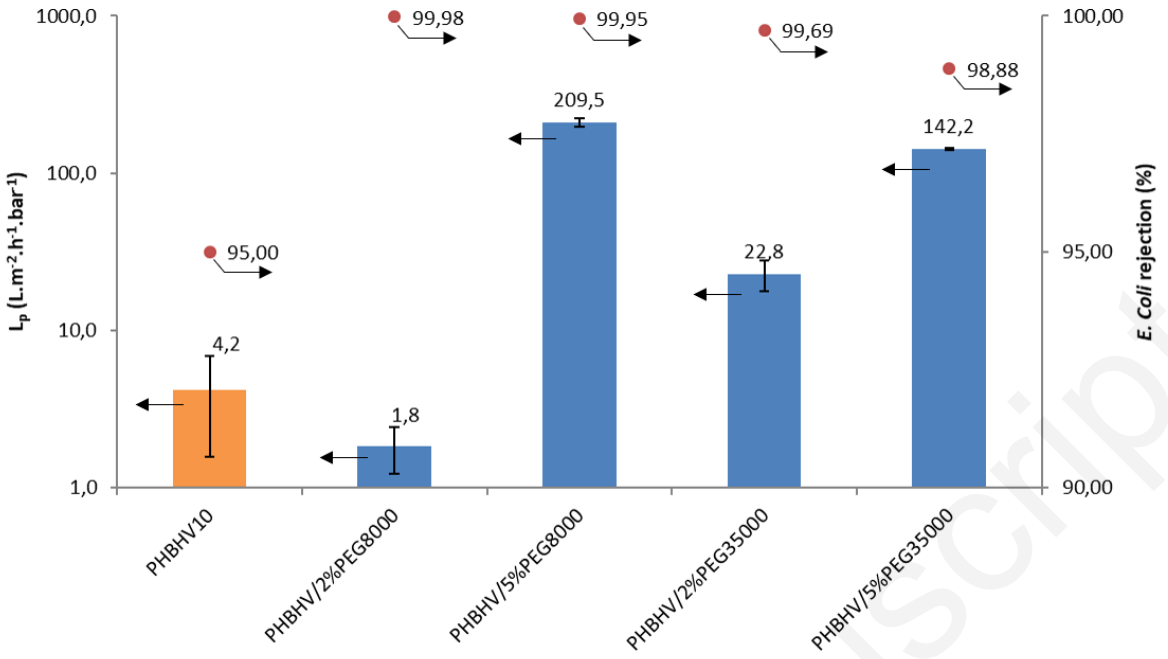

Figure 13 : Pure water permeability and *E. Coli* rejection of the PHBHV membranes with different PEGs as additives.

Similarly to the observations done for PVPs, the addition of PEG8000 or PEG35000 improved the *E. Coli* rejections to roughly 99%. When PEG8000 and PEG35000 are added, it was previously observed on Figure 12 that the pores size distribution was decreased from 1 µm to values ranging between 0.2 µm and 0.6 µm, what would explain the much better rejections of membranes with PEG8000 and PEG35000. By adding 5 wt% of additives, the permeabilities were greatly improved to 209.5 and 142.2 L m^{-2} h^{-1} bar^{-1}, for PHBHV/5%PEG8000 membrane and PHBHV/5%PEG35000 membrane respectively. These values are getting closer to what is expected from microfiltration membranes, generally 500 L m^{-2} h^{-1} bar^{-1} [83].

To obtain more insights into the structure-performances relationship, the membrane permeabilities have been plotted against structural parameters. Membrane permeability was found to increase with membrane thickness (See supplementary material S4). According to Poiseuille's law, for a given porous structure, the permeability should decrease with increasing thickness. The increase of membrane permeability with membrane thickness thus underline that the different membranes have different structural properties (in addition to different thickness) which was obvious from SEM images and membrane pore size and porosity measurements. However, it was found that the permeabilities can be correlated to the membranes porosities (Figure 14).

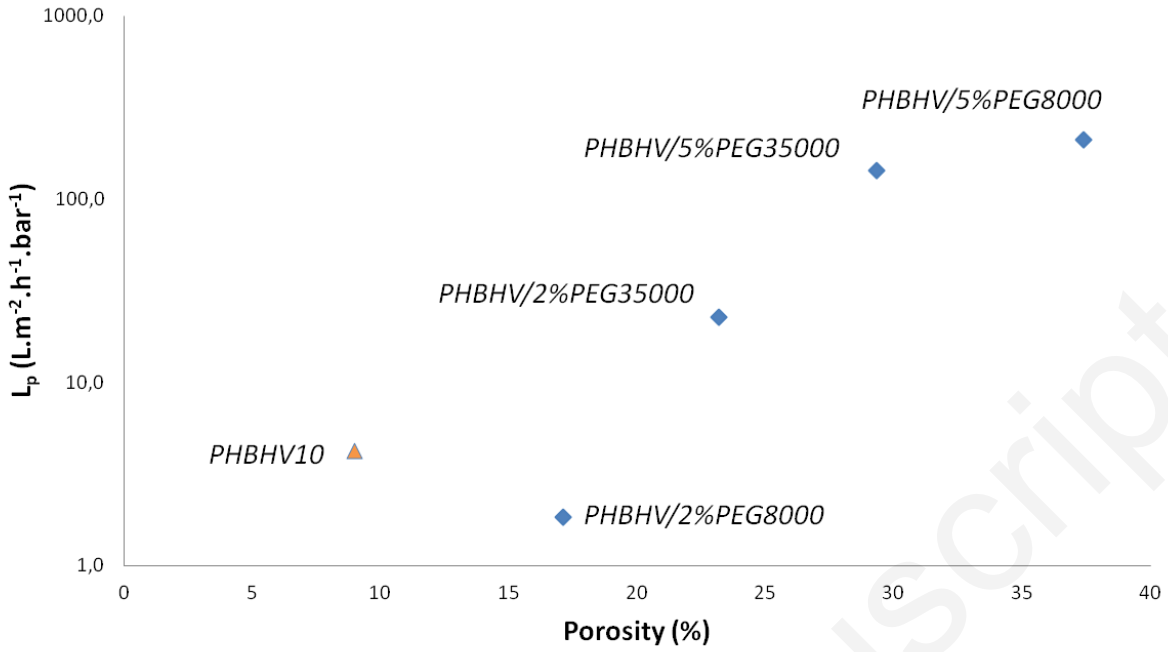

601

602 **Figure 14 : Pure water permeability as a function of the membrane porosity. For membranes with PEGs as additives.**

603 It seems that the porosity strongly influences the permeabilities of these membranes and a higher
604 porosity tends to increase the permeability. However, PHBHV/2%PEG8000 membrane has a higher
605 porosity but smaller permeability compared to membrane PHBHV. It could be explained by the
606 decrease of the pore size distribution leading to a presumably more tortuous (influence of pore
607 tortuosity) water pathway and hence having an opposite effect on the permeability.

608 So far, the addition of these PEGs with the proper molecular weight and concentration seems to be
609 an efficient way to enhance the performances, both the rejection and the permeability, of PHBHV
610 based MF membranes produced by EIPS. The relatively modest pure water permeability compared to
611 commercial MF membranes (in the range 20-10,000 L h^{-1} m^{-2} bar^{-1}, [84]) can be explained by the
612 relatively low porosity of the membrane fabricated in this study (5 – 37 %) compared to commercial
613 MF membranes (65 – 85 %) [85]. However, this study demonstrates the potential of PHBHV, a
614 biobased/biodegradable polymer, as a new material for microfiltration membrane synthesis.

615 4. Conclusion

616 Biobased PHBHV membranes were successfully produced by phase inversion induced by evaporation
617 and tested for MF applications. The structure-performance relationship was, for this first time,
618 studied for membranes made of this biopolymer. Different type of additives, PVPs and PEGs, with
619 different molecular weights and concentrations were added in order to tune the membrane
620 structures and performances. The studied PVPs were able to increase the membrane permeability
621 and *E. Coli* rejection. This improvement was due to the non-solvent effect of the additives which
622 favors the formation of pores. Nevertheless, it was demonstrated that PVP10000 remains more in
623 the final membrane matrix than PVP40000, what makes PVP40000 a slightly better pore former
624 agent. On the other hand, adding PEGs in PHBHV based membranes will have different effects
625 depending of the PEG molecular weight. Since the PEGs have good chemical affinities with the
626 PHBHV matrix, the PEGs with low molecular weights, such as PEG300, will not act as non-solvent and

will hinder the formation of pores. However, the steric hindrance starts to counter balance the chemical affinity in case of PEG8000 and PEG35000, hence these additives act as non-solvents and favor the formation of pores. The performances are strongly correlated to the membrane porosity and pore size. Finally, the membrane with PEG8000 show the best performances so far, with pure water permeabilities over 200 L m^{-2} h^{-1} bar^{-1} associated to the bacteria rejection of 99.95%, what makes it promising for MF applications. The next step of this research work would be to replace the chloroform, herein used as solvent, by a greener alternative in order to make the membrane fabrication process more sustainable.

5. Conflicts of interest

There are no conflicts to declare.

6. Acknowledgements

Francis Gouttefangeas and Loïc Joanny are acknowledged for SEM images performed at CMEBA (ScanMAT, University of Rennes 1) which received a financial support from the European Union (CPER-FEDER 2007-2014). Dr. Audrey Cabrol is acknowledged for her valuable technical advices. Dr. Sylvain Giraudet is acknowledged for is assistance for pore size distribution determination.

7. Notes and References

[1] F. Macedonio, E. Drioli, Membrane Engineering for Green Process Engineering, Engineering. 3 (2017) 290–298. https://doi.org/10.1016/J.ENG.2017.03.026.

[2] J. Hennessy, A. Livingston, R. Baker, Membranes from academia to industry, Nat. Mater. 16 (2017) 280–282. https://doi.org/10.1038/nmat4861.

[3] The future of plastic, Nat. Commun. 9 (2018). https://doi.org/10.1038/s41467-018-04565-2.

[4] J. Gigault, B. Pedrono, B. Maxit, A. ter halle, Marine plastic litter: The unanalyzed nano-fraction, Environ. Sci. Nano. 3 (2016).

[5] Y. Zhu, C. Romain, C.K. Williams, Sustainable polymers from renewable resources, Nature. 540 (2016) 354–362. https://doi.org/10.1038/nature21001.

[6] S. Jiang, B.P. Ladewig, Green synthesis of polymeric membranes: recent advances and future prospects, Curr. Opin. Green Sustain. Chem. 21 (2019) 1–8. https://doi.org/10.1016/J.COGSC.2019.07.002.

[7] F. Galiano, K. Briceño, T. Marino, A. Molino, K.V. Christensen, A. Figoli, Advances in biopolymer-based membrane preparation and applications, J. Memb. Sci. 564 (2018) 562–586. https://doi.org/10.1016/J.MEMSCI.2018.07.059.

[8] K. Keawsupsak, A. Jaiyu, J. Pannoi, P. Somwongsa, N. Wanthausk, P. Sueprasita, C. Eamchotchawalit, Poly(lactic acid)/Biodegradable Polymer Blend for The Preparation of Flat-

664 Sheet Membrane, J. Teknol. 69 (2014). https://doi.org/10.11113/jt.v69.3405.

665 [9] J.P. Chaudhary, S.K. Nataraj, A. Gogda, R. Meena, Bio-based superhydrophilic foam
666 membranes for sustainable oil-water separation, Green Chem. (2014) 4552–4558.
667 https://doi.org/10.1039/c4gc01070a.

668 [10] V.K. Thakur, S.I. Voicu, Recent advances in cellulose and chitosan based membranes for water
669 purification: A concise review, Carbohydr. Polym. 146 (2016) 148–165.
670 https://doi.org/10.1016/j.carbpol.2016.03.030.

671 [11] K.P. Lee, T.C. Arnot, D. Mattia, A review of reverse osmosis membrane materials for
672 desalination—Development to date and future potential, J. Memb. Sci. 370 (2011) 1–22.
673 https://doi.org/10.1016/J.MEMSCI.2010.12.036.

674 [12] E. Saljoughi, T. Mohammadi, Cellulose acetate (CA)/polyvinylpyrrolidone (PVP) blend
675 asymmetric membranes: Preparation, morphology and performance, Desalination. 249 (2009)
676 850–854. https://doi.org/10.1016/j.desal.2008.12.066.

677 [13] B.S. Lalia, V. Kochkodan, R. Hashaikeh, N. Hilal, A review on membrane fabrication: Structure,
678 properties and performance relationship, Desalination. 326 (2013) 77–95.
679 https://doi.org/10.1016/j.desal.2013.06.016.

680 [14] P. Das, S.K. Ray, Synthesis and characterization of biopolymer based mixed matrix membranes
681 for pervaporative dehydration, Carbohydr. Polym. 103 (2014) 274–284.
682 https://doi.org/10.1016/j.carbpol.2013.12.049.

683 [15] A.L. Ahmad, N.M. Yusuf, B.S. Ooi, Preparation and modification of poly (vinyl) alcohol
684 membrane: Effect of crosslinking time towards its morphology, Desalination. 287 (2012) 35–
685 40. https://doi.org/10.1016/J.DESAL.2011.12.003.

686 [16] T. Tanaka, D.R. Lloyd, Formation of poly(l-lactic acid) microfiltration membranes via thermally
687 induced phase separation, J. Memb. Sci. 238 (2004) 65–73.
688 https://doi.org/10.1016/J.MEMSCI.2004.03.020.

689 [17] A.C. Chinyerenwa, H. Wang, Q. Zhang, Y. Zhuang, K.H. Munna, C. Ying, H. Yang, W. Xu,
690 Structure and thermal properties of porous polylactic acid membranes prepared via phase
691 inversion induced by hot water droplets, Polymer (Guildf). 141 (2018) 62–69.
692 https://doi.org/10.1016/J.POLYMER.2018.03.011.

693 [18] Z. Xiong, H. Lin, F. Liu, X. Yu, Y. Wang, Y. Wang, A new strategy to simultaneously improve the
694 permeability , heat- deformation resistance and antifouling properties of polylactide
695 membrane via bio-based β -cyclodextrin and surface crosslinking, J. Memb. Sci. 513 (2016)
696 166–176. https://doi.org/10.1016/j.memsci.2016.04.036.

697 [19] Q. Xing, X. Dong, R. Li, H. Yang, C.C. Han, D. Wang, Morphology and performance control of
698 PLLA-based porous membranes by phase separation, Polymer (Guildf). 54 (2013) 5965–5973.
699 https://doi.org/10.1016/j.polymer.2013.08.007.

700 [20] Keita Kashima and Masanao Imai, Advanced Membrane Material from Marine Biological
701 Polymer and Sensitive Molecular-Size Recognition for Promising Separation Technology, in:
702 Adv. Desalin., 2012: p. 224. https://doi.org/dx.doi.org/10.5772/50734.

703 [21] F. Liu, B. Qin, L. He, R. Song, Novel starch/chitosan blending membrane: Antibacterial,
704 permeable and mechanical properties, Carbohydr. Polym. 78 (2009) 146–150.
705 https://doi.org/10.1016/J.CARBPOL.2009.03.021.

[22] F. Suzuki, H. Kimura, T. Shibue, Formation having a tanning gradient structure of collagen membrane by the pervaporation technique, J. Memb. Sci. 165 (2000) 169–175. https://doi.org/10.1016/S0376-7388(99)00233-1.

[23] P. Wu, M. Imai, Novel Biopolymer Composite Membrane Involved with Selective Mass Transfer and Excellent Water Permeability, in: Adv. Desalin., 2012: p. 224. https://doi.org/10.5772/50697.

[24] T.C. Mokhena, A.S. Luyt, Development of multifunctional nano/ultrafiltration membrane based on a chitosan thin film on alginate electrospun nanofibres, J. Clean. Prod. 156 (2017) 470–479. https://doi.org/10.1016/j.jclepro.2017.04.073.

[25] F. Liu, B. Qin, L. He, R. Song, Novel starch/chitosan blending membrane: Antibacterial, permeable and mechanical properties, Carbohydr. Polym. 78 (2009) 146–150. https://doi.org/10.1016/J.CARBPOL.2009.03.021.

[26] A. Steinbüchel, S. Hein, Biochemical and Molecular Basis of Microbial Synthesis of Polyhydroxyalkanoates in Microorganisms, Adv. Biochem. Eng. 71 (2001) 81–123. https://doi.org/10.1007/3-540-40021-4_3.

[27] R.A.J. Verlinden, D.J. Hill, M.A. Kenward, C.D. Williams, I. Radecka, Bacterial synthesis of biodegradable polyhydroxyalkanoates, J. Appl. Microbiol. 102 (2007) 1437–1449. https://doi.org/10.1111/j.1365-2672.2007.03335.x.

[28] S. Modi, K. Koelling, Y. Vodovotz, Assessment of PHB with varying hydroxyvalerate content for potential packaging applications, Eur. Polym. J. 47 (2011) 179–186. https://doi.org/10.1016/j.eurpolymj.2010.11.010.

[29] Y.M. Corre, S. Bruzaud, J.L. Audic, Y. Grohens, Morphology and functional properties of commercial polyhydroxyalkanoates: A comprehensive and comparative study, Polym. Test. 31 (2012) 226–235. https://doi.org/10.1016/j.polymertesting.2011.11.002.

[30] L. Shen, J. Haufe, M.K. Patel, Product overview and market projection of emerging bio-based plastics, 2009. www.chem.uu.nl/nwswww.copernicus.uu.nlcommissionedbyEuropeanPolysaccharideNetworkofExcellence (accessed May 20, 2019).

[31] A. Elain, A. Le Grand, Y.M. Corre, M. Le Fellic, N. Hachet, V. Le Tilly, P. Loulergue, J.L. Audic, S. Bruzaud, Valorisation of local agro-industrial processing waters as growth media for polyhydroxyalkanoates (PHA) production, Ind. Crops Prod. 80 (2016) 1–5. https://doi.org/10.1016/j.indcrop.2015.10.052.

[32] Tepha Inc., Medical devices and applications of polyhydroxyalkanoate polymers, US7553923B2, 2009. https://patentimages.storage.googleapis.com/1c/9e/0c/1cfbe75517ca50/US7553923.pdf (accessed July 19, 2019).

[33] A. Shrivastav, H.-Y. Kim, Y.-R. Kim, Advances in the applications of polyhydroxyalkanoate nanoparticles for novel drug delivery system., Biomed Res. Int. (2013). https://doi.org/10.1155/2013/581684.

[34] G.-Q. Chen, Q. Wu, The application of polyhydroxyalkanoates as tissue engineering materials, Biomaterials. 26 (2005) 6565–6578. https://doi.org/10.1016/J.BIOMATERIALS.2005.04.036.

[35] P.E. Grimes, B.A. Green, R.H. Wildnauer, B.L. Edison, The use of polyhydroxy acids (PHAs) in

photoaged skin., Cutis. 73 (2004) 3–13. http://www.ncbi.nlm.nih.gov/pubmed/15002656 (accessed July 23, 2019).

[36] L. Hartley Yee, L.J. Ray Foster, Polyhydroxyalkanoates as Packaging Materials: Current Applications and Future Prospects, in: Polyhydroxyalkanoate Based Blends, Compos. Nanocomposites, Royal Society of Chemistry, 2014: pp. 183–207. https://doi.org/10.1039/9781782622314-00183.

[37] A.M. Díez-Pascual, A.L. Díez-Vicente, ZnO-Reinforced Poly(3-hydroxybutyrate- *co* -3-hydroxyvalerate) Bionanocomposites with Antimicrobial Function for Food Packaging, ACS Appl. Mater. Interfaces. 6 (2014) 9822–9834. https://doi.org/10.1021/am502261e.

[38] E. Bugnicourt, P. Cinelli, A. Lazzeri, V. Alvarez, Polyhydroxyalkanoate (PHA): Review of synthesis, characteristics, processing and potential applications in packaging, Express Polym. Lett. 8 (2014) 791–808. https://doi.org/10.3144/expresspolymlett.2014.82.

[39] P. Ragaert, M. Buntinx, C. Maes, C. Vanheusden, R. Peeters, S. Wang, D.R. D'hooge, L. Cardon, Polyhydroxyalkanoates for Food Packaging Applications, in: Ref. Modul. Food Sci., Elsevier, 2019. https://doi.org/10.1016/B978-0-08-100596-5.22502-X.

[40] Buggi Toys GmbH, toy building block, DE102010004338A1, 2010. https://patents.google.com/patent/DE102010004338A1/en (accessed July 19, 2019).

[41] G.-Q. Chen, A microbial polyhydroxyalkanoates (PHA) based bio- and materials industry, Chem. Soc. Rev. 38 (2009) 2434. https://doi.org/10.1039/b812677c.

[42] T. Tsuge, Metabolic improvements and use of inexpensive carbon sources in microbial production of polyhydroxyalkanoates, J. Biosci. Bioeng. 94 (2002) 579–584. https://doi.org/10.1016/S1389-1723(02)80198-0.

[43] Z. Li, J. Yang, X.J. Loh, Polyhydroxyalkanoates : opening doors for a sustainable future, NPG Asia Mater. 8 (2016) e265. https://doi.org/10.1038/am.2016.48.

[44] J. Guo, Q. Zhang, Z. Cai, K. Zhao, Preparation and dye filtration property of electrospun polyhydroxybutyrate–calcium alginate/carbon nanotubes composite nanofibrous filtration membrane, Sep. Purif. Technol. 161 (2016) 69–79. https://doi.org/10.1016/J.SEPPUR.2016.01.036.

[45] A. Nicosia, W. Gieparda, J. Foksowicz-Flaczyk, J. Walentowska, D. Wesołek, B. Vazquez, F. Prodi, F. Belosi, Air filtration and antimicrobial capabilities of electrospun PLA/PHB containing ionic liquid, Sep. Purif. Technol. 154 (2015) 154–160. https://doi.org/10.1016/j.seppur.2015.09.037.

[46] A. Mas, J. Sledz, F. Schue, Membranes en polyhydroxybutyrate et poly(hydroxybutyrate-co-hydroxyvalerate) pour la microfiltration: Influence du non-solvant sur les propriétés hydrodynamiques, Eur. Polym. J. 32 (1996) 427–433. https://doi.org/10.1016/0014-3057(96)80012-7.

[47] A. Mas, H. Jaaba, J. Sledz, F. Schue, Membranes en PHB, P(HB-co-9% HV), P(HB-co-22% HV) pour la microfiltration ou la pervaporation propriétés filtrantes et état de surface, Eur. Polym. J. 32 (1996) 435–450.

[48] M. Villegas, A.I. Romero, M.L. Parentis, E.F. Castro Vidaurre, J.C. Gottifredi, Acrylic acid plasma polymerized poly(3-hydroxybutyrate) membranes for methanol/MTBE separation by pervaporation, Chem. Eng. Res. Des. 109 (2016) 234–248.

https://doi.org/10.1016/J.CHERD.2016.01.018.

[49] M. Villegas, E.F. Castro, A.C. Habert, J.C. Gottifredi, Sorption and pervaporation with poly (3-hydroxybutyrate) membranes : methanol / methyl tertbutyl ether mixtures, J. Memb. Sci. 367 (2011) 103–109. https://doi.org/10.1016/j.memsci.2010.10.051.

[50] J. Guo, Q. Zhang, Z. Cai, K. Zhao, Preparation and dye filtration property of electrospun polyhydroxybutyrate-calcium alginate/carbon nanotubes composite nanofibrous filtration membrane, Sep. Purif. Technol. 161 (2016) 69–79. https://doi.org/10.1016/j.seppur.2016.01.036.

[51] F.E. Ahmed, B.S. Lalia, R. Hashaikeh, A review on electrospinning for membrane fabrication: Challenges and applications, Desalination. 356 (2015) 15–30. https://doi.org/10.1016/j.desal.2014.09.033.

[52] W.L. Tan, N.N. Yaakob, A. Zainal Abidin, M. Abu Bakar, N.H.H. Abu Bakar, Metal Chloride Induced Formation of Porous Polyhydroxybutyrate (PHB) Films : Morphology , Thermal Properties and Crystallinity, IOP Conf. Ser. Mater. Sci. Eng. 133 (2016). https://doi.org/10.1088/1757-899X/133/1/012012.

[53] T.R. Shamala, M.S. Divyashree, R. Davis, K.S.L. Kumari, S.V.N. Vijayendra, B. Raj, Production and characterization of bacterial polyhydroxyalkanoate copolymers and evaluation of their blends by fourier transform infrared spectroscopy and scanning electron microscopy., Indian J. Microbiol. 49 (2009) 251–8. https://doi.org/10.1007/s12088-009-0031-z.

[54] N. Follain, C. Chappey, E. Dargent, F. Chivrac, R. Crétois, S. Marais, Structure and Barrier Properties of Biodegradable Polyhydroxyalkanoate Films, J. Phys. Chem. 118 (2014) 6165–6177.

[55] T. Marino, F. Russo, A. Criscuoli, A. Figoli, TamiSolve ® NxG as novel solvent for polymeric membrane preparation, J. Memb. Sci. 542 (2017) 418–429. https://doi.org/10.1016/j.memsci.2017.08.038.

[56] R.A. Milescu, C.R. Mcelroy, T.J. Farmer, P.M. Williams, M.J. Walters, J.H. Clark, Z. Xie, Fabrication of PES/PVP Water Filtration Membranes Using Cyrene, a Safer Bio-Based Polar Aprotic Solvent, Adv. Microb. Physiol. (2019). https://doi.org/10.1155/2019/9692859.

[57] D.W. van (Dirk W. Krevelen, K. te. Nijenhuis, Properties of polymers : their correlation with chemical structure ; their numerical estimation and prediction from additive group contributions, Elsevier, 2009.

[58] C. Özdemir, A. Güner, Solubility profiles of poly(ethylene glycol)/solvent systems, I: Qualitative comparison of solubility parameter approaches, Eur. Polym. J. 43 (2007) 3068–3093. https://doi.org/10.1016/j.eurpolymj.2007.02.022.

[59] N. Galego, F.C. Miguens, R. Sánchez, Physical and functional characterization of PHA SCL membranes, Polymer (Guildf). 43 (2002) 3109–3114.

[60] T. Phaechamud, S. Chitrattha, Pore formation mechanism of porous poly(dl-lactic acid) matrix membrane, Mater. Sci. Eng. C. 61 (2016) 744–752. https://doi.org/10.1016/j.msec.2016.01.014.

[61] H.-S. Huag, S.-H. Chou, T.-M. Don, W.-C. Lai, L.-P. Cheng, Formation of microporous poly(hydroxybutyric acid) membranes for culture of osteoblast and fibroblast, Polym. Adv. Technol. 20 (2009) 1082–1090. https://doi.org/10.1002/pat.1366.

[62] J.-H. Kim, K.-H. Lee, Effect of PEG additive on membrane formation by phase inversion, J. Memb. Sci. 138 (1998) 153–163. https://doi.org/10.1016/S0376-7388(97)00224-X.

[63] A. Idris, N. Mat Zain, M.Y. Noordin, Synthesis, characterization and performance of asymmetric polyethersulfone (PES) ultrafiltration membranes with polyethylene glycol of different molecular weights as additives, Desalination. 207 (2007) 324–339. https://doi.org/10.1016/j.desal.2006.08.008.

[64] B. Chakrabarty, A.K. Ghoshal, M.K. Purkait, Preparation, characterization and performance studies of polysulfone membranes using PVP as an additive, J. Memb. Sci. 315 (2008) 36–47. https://doi.org/10.1016/j.memsci.2008.02.027.

[65] M. Amirilargani, T. Mohammadi, Effects of PEG on morphology and permeation properties of polyethersulfone membranes, Sep. Sci. Technol. 44 (2009) 3854–3875. https://doi.org/10.1080/01496390903182347.

[66] B. Chakrabarty, A.K. Ghoshal, M.K. Purkait, Effect of molecular weight of PEG on membrane morphology and transport properties, J. Memb. Sci. 309 (2008) 209–221. https://doi.org/10.1016/j.memsci.2007.10.027.

[67] S. Rekha Panda, S. De, Role of polyethylene glycol with different solvents for tailor-made polysulfone membranes, J. Polym. Res. 20 (2013). https://doi.org/10.1007/s10965-013-0179-4.

[68] A. Urkiaga, D. Iturbe, J. Etxebarria, Effect of different additives on the fabrication of hydrophilic polysulfone ultrafiltration membranes, Desalin. Water Treat. 56 (2015) 3415–3426. https://doi.org/10.1080/19443994.2014.1000976.

[69] R. Pervin, P. Ghosh, M.G. Basavaraj, Tailoring pore distribution in polymer films via evaporation induced phase separation, RSC Adv. 9 (2019) 15593–15605. https://doi.org/10.1039/c9ra01331h.

[70] R.K. Arya, Drying Induced Phase Separation, 2012. https://pdfs.semanticscholar.org/ceda/6b7ad05044e8ef531344dafcdf8cece13651.pdf (accessed June 18, 2019).

[71] S. Randriamahefa, E. Renard, P. Guérin, V. Langlois, Fourier Transform Infrared Spectroscopy for Screening and Quantifying Production of PHAs by *Pseudomonas* Grown on Sodium Octanoate, Biomacromolecules. 4 (2003) 1092–1097. https://doi.org/10.1021/bm034104o.

[72] Y. Hanafi, A. Szymczyk, M. Rabiller-Baudry, K. Baddari, Degradation of Poly(Ether Sulfone)/Polyvinylpyrrolidone Membranes by Sodium Hypochlorite: Insight from Advanced Electrokinetic Characterizations, Environ. Sci. Technol. 48 (2014) 13419–13426. https://doi.org/10.1021/es5027882.

[73] D. Wang, K. Li, W.K. Teo, Preparation and characterization of polyvinylidene fluoride (PVDF) hollow fiber membranes, J. Memb. Sci. 163 (1999) 211–220. https://doi.org/10.1016/S0376-7388(99)00181-7.

[74] S.-G. Hong, T.-K. Gau, S.-C. Huang, Enhancement of the crystallization and thermal stability of polyhydroxybutyrate by polymeric additives, J. Therm. Anal. Calorim. 103 (2011) 967–975. https://doi.org/10.1007/s10973-010-1180-3.

[75] G. Reshes, S. Vanounou, I. Fishov, M. Feingold, Cell shape dynamics in Escherichia coli., Biophys. J. 94 (2008) 251–64. https://doi.org/10.1529/biophysj.107.104398.

874 [76] Y. Ma, F. Shi, J. Ma, M. Wu, J. Zhang, C. Gao, Effect of PEG additive on the morphology and
875 performance of polysulfone ultrafiltration membranes, Desalination. 272 (2011) 51–58.
876 https://doi.org/10.1016/J.DESAL.2010.12.054.

877 [77] Z.L. Xu, T.S. Chung, K.C. Loh, B.C. Lim, Polymeric asymmetric membranes made from
878 polyetherimide/polybenzimidazole/poly(ethylene glycol) (PEI/PBI/PEG) for oil-surfactant-
879 water separation, J. Memb. Sci. 158 (1999) 41–53. https://doi.org/10.1016/S0376-
880 7388(99)00030-7.

881 [78] D.F. Parra, J. Fusaro, F. Gaboardi, D.S. Rosa, Influence of poly (ethylene glycol) on the thermal,
882 mechanical, morphological, physical–chemical and biodegradation properties of poly (3-
883 hydroxybutyrate), Polym. Degrad. Stab. 91 (2006) 1954–1959.
884 https://doi.org/10.1016/j.polymdegradstab.2006.02.008.

885 [79] R. Requena, A. Jiménez, M. Vargas, A. Chiralt, Effect of plasticizers on thermal and physical
886 properties of compression-moulded poly[(3-hydroxybutyrate)-co-(3-hydroxyvalerate)] films,
887 Polym. Test. 56 (2016) 45–53. https://doi.org/10.1016/J.POLYMERTESTING.2016.09.022.

888 [80] B. Liu, Q. Du, Y. Yang, The phase diagrams of mixtures of EVAL and PEG in relation to
889 membrane formation, J. Memb. Sci. 180 (2000) 81–92. https://doi.org/10.1016/S0376-
890 7388(00)00526-3.

891 [81] E. Fekete, E. Földes, B. Pukánszky, Effect of molecular interactions on the miscibility and
892 structure of polymer blends, Eur. Polym. J. 41 (2005) 727–736.
893 https://doi.org/10.1016/j.eurpolymj.2004.10.038.

894 [82] J. Zhao, G. Luo, J. Wu, H. Xia, Preparation of Microporous Silicone Rubber Membrane with
895 Tunable Pore Size via Solvent Evaporation-Induced Phase Separation, ACS Appl. Mater.
896 Interfaces. 5 (2013) 2040–2046. https://doi.org/10.1021/am302929c.

897 [83] N. Hilal, A.F. Ismail, C.J. Wright, Membrane fabrication, 2018.

898 [84] M.R. Landsman, R. Sujanani, S.H. Brodfuehrer, C.M. Cooper, A.G. Darr, R.J. Davis, K. Kim, S.
899 Kum, L.K. Nalley, S.M. Nomaan, C.P. Oden, A. Paspureddi, K.K. Reimund, L.S. Rowles, S. Yeo,
900 D.F. Lawler, B.D. Freeman, L.E. Katz, Water Treatment: Are Membranes the Panacea?, Annu.
901 Rev. Chem. Biomol. Eng. 11 (2020) 559–585. https://doi.org/10.1146/annurev-chembioeng-
902 111919-091940.

903 [85] H. Feroz, M. Bai, H. Kwon, J. Brezovec, J. Peng, M. Kumar, Can Fibrous Mats Outperform
904 Current Ultrafiltration and Microfiltration Membranes?, Ind. Eng. Chem. Res. 56 (2017)
905 10438–10447. https://doi.org/10.1021/acs.iecr.7b01351.

906